1

Multiband OFDM Modulation and Demodulation for Ultra Wideband Communications

Runfeng Yang[1] and R. Simon Sherratt[2]
[1]*Dongguan Polytechnic*
[2]*University of Reading*
[1]*China,*
[2]*United Kingdom*

1. Introduction

This chapter considers the Multiband Orthogonal Frequency Division Multiplexing (MB-OFDM) modulation and demodulation with the intention to optimize the Ultra-Wideband (UWB) system performance. OFDM is a type of multicarrier modulation and becomes the most important aspect for the MB-OFDM system performance. It is also a low cost digital signal component efficiently using Fast Fourier Transform (FFT) algorithm to implement the multicarrier orthogonality. Within the MB-OFDM approach, the OFDM modulation is employed in each 528 MHz wide band to transmit the data across the different bands while also using the frequency hopping technique across different bands. Each parallel bit stream can be mapped onto one of the OFDM subcarriers.

Quadrature Phase Shift Keying (QPSK) and Dual Carrier Modulation (DCM) are currently used as the modulation schemes for MB-OFDM in the ECMA-368 defined UWB radio platform. A dual QPSK soft-demapper is suitable for ECMA-368 that exploits the inherent Time-Domain Spreading (TDS) and guard symbol subcarrier diversity to improve the receiver performance, yet merges decoding operations together to minimize hardware and power requirements. There are several methods to demap the DCM, which are soft bit demapping, Maximum Likelihood (ML) soft bit demapping, and Log Likelihood Ratio (LLR) demapping. The Channel State Information (CSI) aided scheme coupled with the band hopping information is used as a further technique to improve the DCM demapping performance.

ECMA-368 offers up to 480 Mb/s instantaneous bit rate to the Medium Access Control (MAC) layer, but depending on radio channel conditions dropped packets unfortunately result in a lower throughput. An alternative high data rate modulation scheme termed Dual Circular 32-QAM that fits within the configuration of the current standard increasing system throughput thus maintaining the high rate throughput even with a moderate level of dropped packets.

2. MB-OFDM in ECMA-368

2.1 UWB standardization

The fundamental issue of UWB is that the transmitted signal can be spread over an extremely large bandwidth with very low Power Spectral Density (PSD). In early 2002, the

USA Federal Communications Commission (FCC) agreed to allocate 7500 MHz RF spectrum in 3.1-10.6 GHz band for unlicensed use for the UWB devices (Federal Communications Commission [FCC], 2002a), and limit the UWB Effective Isotropic Radiated Power (EIRP) to -41.3 dBm/MHz (FCC, 2002b). In later 2002, Ellis *et al* (Ellis et al., 2002) published the initial requirements specification for UWB systems.

Many UWB proposals were made to converge on an agreed solution. Two clear candidates quickly emerged under the Institute of Electrical and Electronic Engineering (IEEE) 802.15.3a working party for Wireless Personal Area Network (WPAN), which were Direct-Sequence (DS) UWB (Fisher et al., 2005) and MB-OFDM (Batra, et al., 2004a). In parallel with the IEEE standardization attempted, the Multiband OFDM Alliance Special Interest Group (MBOA-SIG) forged ahead to standardize their UWB system based on MB-OFDM. A key activity in MBOA-SIG development was MB-OFDM being selected by the USB implementers forum for the new Wireless-USB Physical layer (PHY) standard (USB Implementers forum, 2005). In 2005, the WiMedia Alliance working with European Computer Manufacturers Association (ECMA) announced the establishment of the WiMedia MB-OFDM UWB radio platform as their global UWB PHY and Media Access Control (MAC) standard, ECMA-368, based on the previous MBOA-SIG proposal (Multiband OFDM Alliance, 2004) with only minor changes. A third updated version of ECMA-368 was published in December 2008 with additions for regulatory flexibility and maintained as ISO/IEC 26907 (ECMA, 2008).

ECMA-368 specifies an MB-OFDM system occupying 14 bands with a bandwidth of 528 MHz for each band. This technique has the capability to efficiently capture multipath energy with a single RF chain. The first 12 bands are grouped into 4 band groups (BG1-BG4), and the last two bands are grouped into a fifth band group (BG5). A sixth band group (BG6) containing band 9, 10 and 11 is also defined within the spectrum of BG3 and BG4, in agreement to usage within worldwide spectrum regulations. The advantage of the grouping is that the transmitter and receiver can process a smaller bandwidth signal while taking advantages from frequency hopping. Figure 1 depicts the band group allocation.

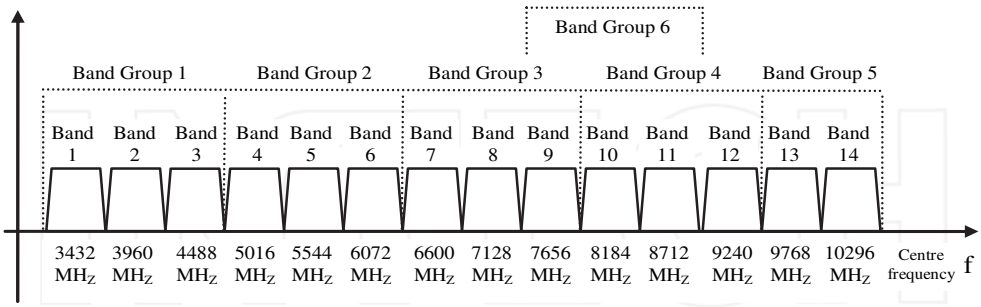

Fig. 1. Band group allocation (ECMA-International, 2008)

2.2 PHY operation in MB-OFDM

To operate the PHY service interface to the MAC, a Physical Layer Convergence Protocol (PLCP) sublayer is defined to provide a method for converting a PSDU (PHY Service Data Unit) into a PPDU (PLCP Packet Data Unit) composed from three components: the PLCP preamble (containing the Packet/Frame Synchronization and the Channel Estimation

sequence), the PLCP header, and the PSDU, as illustrated in Figure 2. They are added with appropriated error detection and correction schemes to robust a communication channel as practically possible. When transmitting the packets, the PLCP preamble is sent first, followed by the PLCP header, and finally the PSDU. At the receiver, the PLCP preamble and PLCP header are processed to aid in the demodulation, decoding and delivery of the PSDU.

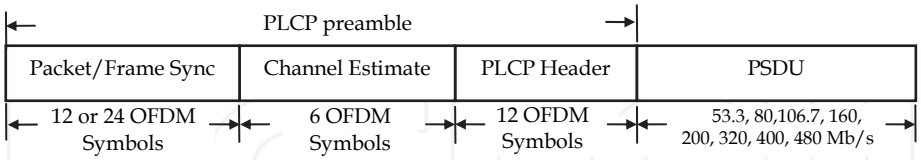

Fig. 2. PPDU structure

To transmit a PSDU that contains the information bits, ECMA-368 has eight transmission modes by applying various levels of coding and diversity to offer 53.3, 80, 106.7, 160, 200, 320, 400 or 480 Mb/s. Firstly the PSDU needs to be scrambled by the scrambler, then it is encoded by puncturing the convolutional code to achieve the appropriate coding rate, 1/3, 1/2, 5/8 or 3/4, interleaved and modulated onto a QPSK complex constellation for data rates 200 Mb/s and lower, or DCM for data rates 320 Mb/s and higher. After bit interleaving, the coded and interleaved binary data sequence is mapped onto a QPSK or DCM complex constellation. The resulting complex numbers are loaded onto the data subcarriers of the OFDM symbol implemented using an IFFT to create real or complex baseband signal. Figure 3 depicts the encoding process for the PSDU at the transmitter.

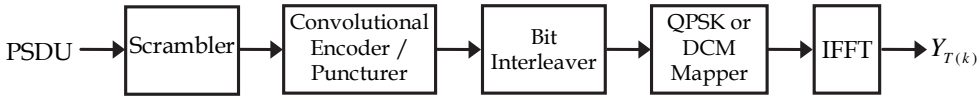

Fig. 3. Encoding process for the PSDU at Transmitter

At the heart of ECMA-368 lies a 128-pt IFFT with a 242.42ns IFFT period resulting in each IFFT subcarrier being clocked at 528MHz. The subcarriers in each OFDM symbol include 100 data subcarriers, 12 pilot subcarriers, 6 NULL valued subcarriers and 10 guard subcarriers. The 10 guard subcarriers used for mitigating Inter Symbol Interference (ISI) are located on either edge of the OFDM symbol and have same value as the 5 outermost data subcarriers. Each OFDM symbol is separated with a Zero Padded Suffix (ZPS) of 70.08ns (37 zeros as the FFT rate) to aid multipath interference mitigation and settling times of the transmitter and receiver. The IFFT/FFT operation ensures that subcarriers do not interfere with one other. Moreover, Frequency-Domain Spreading (FDS) and Time-Domain Spreading (TDS) can be used to obtain further bandwidth expansion within the OFDM modulation process depending on the coding scheme in ECMA-368.

2.3 Frequency hopping

ECMA-368 employs a frequency hopping technique in which the band is hopped by using a Time-Frequency code (TFC) known to both transmitter and receiver. The transceiver transmits a single OFDM symbol in one band, and then the next transmitted OFDM symbol is hopped to the next band. Figure 4 depicts OFDM symbols transmitted in RF signal

utilizing a TFC within Band group 1 (BG1). There are two types of TFCs: Time-Frequency Interleaving (TFI), where the coded information is interleaved over three bands; and Fixed-Frequency Interleaving (FFI), where the coded information is transmitted on a single band. BG1 is a mandatory mode targeted for the first generation UWB devices.

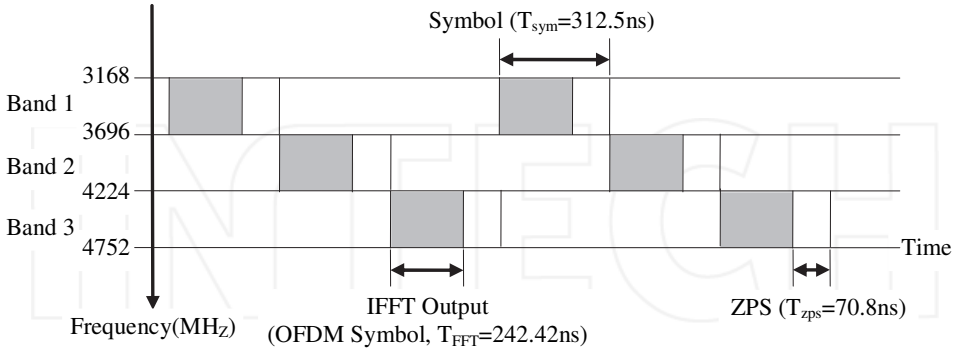

Fig. 4. OFDM symbols transmitted in RF signal utilizing a TFC within BG1

2.4 System performance measurements

Simulating system performance is an important criterion in order to compare to current literature. However, the literature on MB-OFDM system performance for measuring propagation with respect to distance is surprisingly sparse. We followed the original MBOA-SIG MB-OFDM proposal settings and adopted the assumptions (described in the following section 2.4.2) to simulate the MB-OFDM system with standard UWB channels.

2.4.1 Propagation distance measurement

The received signal power is calculated the difference between the total transmit power and path loss. Since the FCC defines the average power as 1mW per Megahertz, the total transmitted power P_{TX} can be obtained from the PSD and the operating bandwidth, as in (1) assuming no power loss at the transmitter and 0 dBi transmit antenna gain.

$$P_{TX} = -41.25 + 10\log_{10}(f_U - f_L) \text{ dBm} \tag{1}$$

where -41.25 dBm/MHz is the UWB EIRP/MHz, f_L = 3168 MHz is the lower frequency of the operating bandwidth, f_U is upper frequency varying from BG1 to BG6. However, BG1 is used for first generation of UWB devices, thus f_U = 4752 MHz is assigned. The free-space propagation model is defined under IEEE 802.15.3a, which specifies the path loss attenuating the transmitted signal as a function of the lower and upper frequencies of the operating bandwidth. The path loss P_L can be expressed as in (2).

$$P_L = 20\log_{10}(\frac{4\pi f_g d}{c}) \text{ dB} \tag{2}$$

where f_g = 3882 MHz is the geometric mean of the lower and upper frequencies in BG1. The geometric mean offers a more reasonable value for the expected path loss in the system (Batra et al., 2004b). d is the distance measured in meters between the transmitter and

receiver. c = 3x108 m/s is the speed of light. As a result, the function of received signal power, as described in (3), can be derived from (1) and (2) with transmit and receive antenna gain (G_T, G_R).

$$P_{RX} = P_{TX} + G_T + G_R - P_L \text{ dBm} \tag{3}$$

2.4.2 Receiver sensitivity

Receiver sensitivity is the lowest power level at which the receiver can detect an RF signal and demodulate data. Sensitivity is purely a receiver specification and is independent of the transmitter. In ECMA-368, the minimum receiver sensitivity values in Additive White Gaussian Noise (AWGN) for different data rates are listed in Table 1 for BG1 to achieve a Packet Error Rate (PER) of less than 8% with a payload of 1024 octets each in the PSDU, where a noise figure of 6.6 dB (referenced at the antenna), an implementation loss of 2.5 dB, and a margin of 3 dB have been assumed (ECMA, 2008).

Data Rate (Mb/s)	Minimum Receiver Sensitivity (dBm)
53.3	-80.8
80	-78.9
106.7	-77.8
160	-75.9
200	-74.5
320	-72.8
400	-71.5
480	-70.4

Table 1. Minimum receiver sensitivities for BG1 (ECMA, 2008)

2.4.3 System configuration

The proposed UWB system is simulated in a realistic multipath channel environment of 100 channel realizations in the four UWB channel models CM1-CM4 (Foerster, 2003). The simulation results are averaged over at least 500 packets with a payload of 1024 octets each in the PSDU and 90th-percentile channel realization (the worst 10% channels are discarded). The link success probability is defined as the 90th-percentile of channel realizations for which system can successfully acquire and demodulate a packet with a PER (a packet is in error if at least one bit is in error) of less than 8% (Multiband OFDM Alliance, 2004).

The original MBOA-SIG proposal specifies implementation loss affecting the practical system, which includes front-end filtering, clipping at the Digital-to-Analogue Converter (DAC), Analogue-to-Digital Converter (ADC) degradation, channel estimation, clock frequency mismatch (±20 ppm at the transmitter and receiver), carrier offset recovery, carrier tracking, etc. Similarly, ECMA-368 specifies the total implementation loss of 2.5 dB and a margin of 3 dB as an assumption. It should be noted that ECMA-368 only defines the

performance for reference sensitivity, not multipath. This research will revert back to multipath test performed in the original MBOA-SIG tests when appropriate.
This research will maintain strict adherence to timing (no frequency offset and perfect OFDM symbol timing) and use a hopping characteristic of TFC = 1, and incorporate 6.6 dB noise figure referenced at the antenna and 2.5 dB implementation loss in the floating point system model. PER being a function of distance will be used as a performance indicator for the system performance measurement.

3. QPSK modulation

3.1 QPSK mapping

QPSK constellation mapping is used when data rate is 200 Mb/s or lower combing with FDS and (or) TDS techniques. The FDS and TDS modes are not only used to create the varied data rates, but also maximize frequency diversity and improve the performance. ECMA-368 offers eight data rates with various levels of coding and diversity to achieve the required trade-off between speed and reliability. For the slowest 5 out of the 8 PSDU coding schemes (summarized in Table 2), or for the PLCP header, the binary coded and interleaved input data are divided into groups of two bits, and then mapped in one of the four Gray-coded QPSK constellation points, as in Figure 5. By mapping two bits per symbol, the output symbol values *Y[k]*, as in (4), are normalized by a normalization factor of K_{MOD} = $1/\sqrt{2}$, to have constant average symbol power.

$$Y[k] = K_{MOD} \times \left[(2 \times b[2k] - 1) + j(2 \times b[2k+1] - 1) \right] \tag{4}$$

where k = 0, 1, 2, …n; n = 49 is used when FDS is enabled, otherwise n = 99.

Data Rate (Mb/s)	Modulation	Coding Rate (R)	FDS	TDS	Coded Bits / 6 OFDM symbol	Info Bits / 6 OFDM symbol
53.3	QPSK	1/3	Yes	Yes	300	100
80	QPSK	1/2	Yes	Yes	300	150
106.7	QPSK	1/3	No	Yes	600	200
160	QPSK	1/2	No	Yes	600	300
200	QPSK	5/8	No	Yes	600	375
320	DCM	1/2	No	No	1200	600
400	DCM	5/8	No	No	1200	750
480	DCM	3/4	No	No	1200	900

Table 2. PSDU rate-dependent parameters (ECMA, 2008)

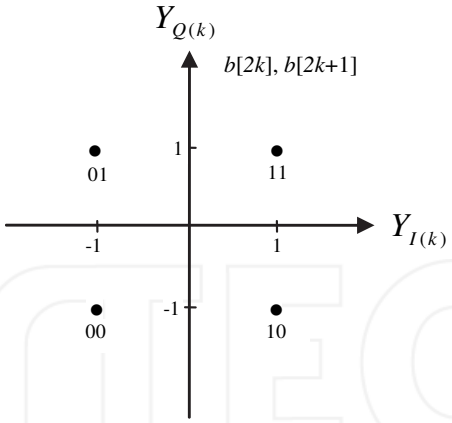

Fig. 5. QPSK constellation mapping

ECMA-368 supports TDS and (or) FDS to provide repetition of the same information (complex number) mapping over the OFDM symbols for the slowest 5 out of the 8 coding schemes. In conjunction with the FDS approach, 50 QPSK symbols and 50 of their respective conjugate values are mapped onto 100 OFDM data subcarriers as conjugate symmetric IFFT inputs. As a result, the transmitter only needs to implement the real portion of the IFFT output. As for the TDS approach, when 100 QPSK symbols are mapped onto an OFDM symbol, the copy of these 100 QPSK symbols is mapped onto the next OFDM symbol.

3.2 A dual QPSK soft-demapper exploiting TDS and guard interval diversity

Soft bit decision is used to demap the QPSK to maximize the post-QPSK baseband processing. However a soft bit based receiver will consume more memory in the deinterleaver and increase the computational complexity of the Viterbi decoder, and it will be required to store the soft bit trackback memory to search the 64 trellis states for each information bit. The soft-QPSK demapping process can improve WPAN receiver performance where each input complex number for the demapper outputs two soft bits being the symbol likelihood. The demapping process can be simply the process of outputting real part (I value) and then the imaginary part (Q value) of the input symbol for the first and second soft bit respectively. For a given code bit, a positive soft bit with large possible magnitude may indicate more confidence in '1' being sent for the code bit, while a negative soft bit with large possible magnitude may indicate more confidence in '0' being sent for the code bit, and a soft bit of zero may indicate equal likelihood of '0' or '1' being sent for the code bit. The soft bits from the QPSK demodulator are then input to the bit deinterleaver, then Viterbi decoder and descrambler to recover the original bit stream, as shown in Figure 6.

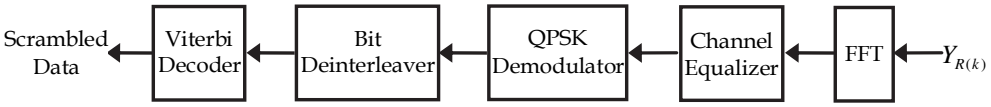

Fig. 6. Decoding process for the PSDU for low data rates or PLCP header at Receiver

3.2.1 Time-domain de-spreading and equal gain combing

As ECMA-368 implements frequency hopping, each time diversity pair in the TDS is transmitted over a different frequency band and therefore has independent channel fading characteristics. The possibility of both OFDM symbols having deep fades on the same subcarriers from different frequency bands is small. The receiver may decide to select and decode one received OFDM symbol or combine the two to maximize performance. Since the duration of an OFDM symbol is fixed, the receiver may implement a single serial decoding path for each symbol pair, or have two parallel decoding paths clocked at half the serial rate. ne main OFDM symbol and its spread OFDM symbol are received at the receiver. After the equalization, the data from those two OFDM symbols are demodulated by QPSK. Since QPSK soft demapping is used for a pair of main and spread QPSK symbols, the receiver must implement soft decision for the soft bit decoding. For two one-dimensional points (x_1, y_1) and (x_2, y_2), the Euclidean distance is computed in (5). The spread decision can be selected from calculating the Euclidean symbol distance between the corresponding QPSK constellation point to a main QPSK symbol, Ym_k, or a spread QPSK symbol, Ys_k, and then output the symbol that has shorter distance. d_m and d_s are the Euclidean distances for Ym_k and Ys_k respectively, as described in (6)-(7). Ym_k and Ys_k are the signals after the equalisation. Figure 7 depicts possible QPSK symbol pairs from the main and spread OFDM symbols.

$$d = \sqrt{(x_2 - x_1)^2 + (y_2 - y_1)^2} \tag{5}$$

$$d_m = \sqrt{\{\mathrm{Re}(Ym_k) - \mathrm{Re}(S_n)\}^2 + \{\mathrm{Im}(Ym_k) - \mathrm{Im}(S_n)\}^2} \tag{6}$$

$$d_s = \sqrt{\{\mathrm{Re}(Ys_k) - \mathrm{Re}(S_n)\}^2 + \{\mathrm{Im}(Ys_k) - \mathrm{Im}(S_n)\}^2} \tag{7}$$

where $k = 0, 1 \ldots 99$; S_n is the reference signal for one of the four constellation points. Then the soft value of Ym_k and Ys_k is used after deciding the Euclidean distance, as the following:

$$Soft(b_{2k}) = \mathrm{Re}(Ym_k) \qquad Soft(b_{2k+1}) = \mathrm{Im}(Ym_k), \quad if\,(d_m < d_s) \tag{8}$$

$$Soft(b_{2k}) = \mathrm{Re}(Ys_k) \qquad Soft(b_{2k+1}) = \mathrm{Im}(Ys_k), \quad if\,(d_s < d_m) \tag{9}$$

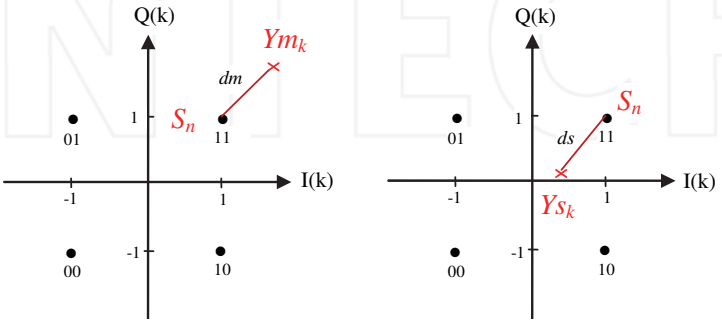

Fig. 7. A possible equalized QPSK symbol pairs from the main and spread OFDM symbols

Equal gain combing scheme can be employed to combine the spread sequence whether before the QPSK demapping process or after the QPSK demapping process. The demapping process can be integrated into the symbol decoding scheme and the combined QPSK soft-demapping and TDS symbol simply reduces to (10) and (11). The overall likelihood of a larger signal to noise ratio value is increased, thereby increasing more reliability for Viterbi decoder input. This equal gain combing scheme not only has better soft decoding performance than the spread decision, but also has much lower complexity.

$$Soft(b_{2k}) = \mathrm{Re}(Ym_k) + \mathrm{Re}(Ys_k) \quad k = 0, 1, \ldots 99 \tag{10}$$

$$Soft(b_{2k+1}) = \mathrm{Im}(Ym_k) + \mathrm{Im}(Ys_k) \tag{11}$$

3.2.2 Merged TDS and QPSK soft demapping architecture

Merging the TDS and QPSK soft-demapper architecture can be used to optimize the receiver performance. At the rates where TDS is implemented, the receiver architecture can process the main and spread OFDM symbols in parallel (to reduce hardware, but clock rates are often high). In this proposed dual QPSK soft-demapper, the parallel approach is assumed, as illustrated in Figure 8, but the serial approach can also be used where additional memory for holding one equalizer output buffer is required before the two equalized symbols are merged. The main and spread symbols have their own FFT and equalizer in the parallel implementation. This may be considered as a consumptive resource solution, because too much dynamic range is expensive in terms of power and floor size, particularly for the FFT. To implement the demapping and combining process, the basic operations include fetching I and Q values, add, shift, and store. The proposed dual QPSK demapper requires no memory to hold the QPSK demapping output before the add operation. Thus a reduction of 40% required memory has been achieved compared to having separate demapping and combining functions. The dual soft-QPSK demapping process and the management of guard subcarriers are implemented with zero overhead.

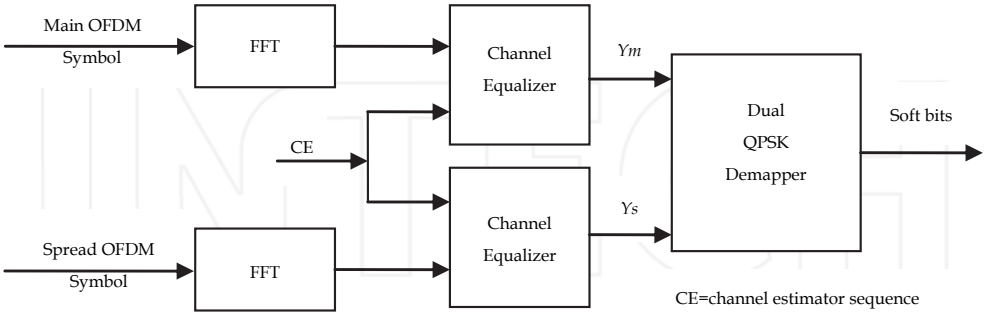

Fig. 8. Architecture of soft-output QPSK demapper with TDS symbol combining

3.2.3 Use of guard subcarrier diversity

In ECMA-368, an OFDM symbol contains 100 data subcarriers ($C_d[0..99]$), 10 guard subcarriers ($C_g[0..9]$), 12 pilot subcarriers ($C_p[0..11]$) and 6 Null subcarriers. The 10 guard

subcarriers are aimed at minimizing ISI and are split into 2 sets of 5 carriers each set at either end of the IFFT input data set, and they are the same values as the 5 neighbouring data subcarriers. The power can be reduced on the guard subcarriers with the objective to relax the specifications of the analogue transmit and receive filters.

The guard subcarriers can be considered as another form of time and frequency diversity, at least to the 2 sets of 5 neighbouring data subcarriers, to improve the performance of the receiver. In this case, each of the 5 outer data subcarriers ($C_d[0..4]$ and $C_d[95..99]$) are computed as the sum of the data subcarriers and its associated guard subcarriers ($C_g[0..4]$ and $C_g[5..9]$), as described in (12). There are many Maximum Ratio Combing (MRC) (Proakis, 2001) schemes to utilize the guard subcarriers as another form of the diversity, but they are difficult to implement while considering the high data rate in ECMA-368, hence implementing as the sum of the data can simplify the computation and decoding process at the receiver, as described in the following:

$$C_d[k] = C_d[k] + C_g[n] \text{ , k = 0, 1, 2, 3, 4; n = 0, 1, 2, 3, 4} \quad (12)$$

$$C_d[k] = C_d[k] + C_g[n] \text{ , k = 95, 96, 97, 98, 99; n = 5, 6, 7, 8, 9}$$

3.2.4 Performance gain by exploiting guard interval diversity

By following system configuration stated in section 2.4.3, the system was simulated with exploiting guard interval diversity in conjunction with merged TDS and QPSK soft demapping architecture in the 200 Mb/s mode. Two models are presented here, an AWGN channel and channel realisation 1 in CM1. The simulation was performed both with the use of guard subcarriers and without the use of the guard subcarriers. Figure 9 depicts the performance gains in the order of 0.3 dB for utilizing the received guard symbols. At UWB frequencies of BG 1, FCC compliant transmitter power and expected distance of 10 meters then the 0.3 dB improvement equates to a propagation distance improvement to 10.4 meters.

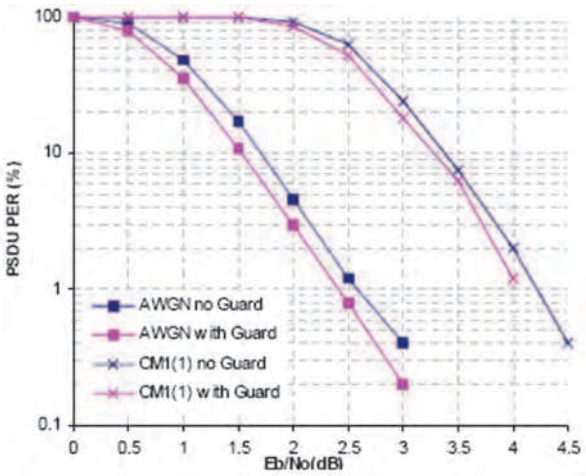

Fig. 9. PSDU PER Performance improvement from utilizing guard interval diversity in the AWGN and Channel realization 1 in CM1

3.2.5 System performance for 200 Mb/s mode

The system performance at a data rate of 200 Mb/s is simulated with using the UWB channel models to measure propagation distance. The proposed dual QPSK soft-demapper with TDS mode and guard interval diversity is used in the simulation. To obtain more accurate simulation results, 2000 packets per simulation with a payload of 1024 octets were used in each PSDU and 90th-percentile channel realization, including a noise figure of 6.6 dB and an implementation loss of 2.5 dB. The other settings remained the same as before. The system using the 200 Mb/s mode can achieve a successful link of 9.7 meters in CM1, and 9.8 meters in CM3, as illustrated in Figure 10. This performance has supported the WiMedia requirements for the extended distances of about 10 meters at the lower data rates. It is imperative to compare the system performance with current literature. As illustrated in Figure 11, the proposed system for the 200 Mb/s mode in CM1 has a better performance, while MBOA-SIG quoted 7.4 meters (Multiband OFDM Alliance, 2004) and 6.8 meters from aRenarti semiconductor (aRenarti Semiconductor, 2007).

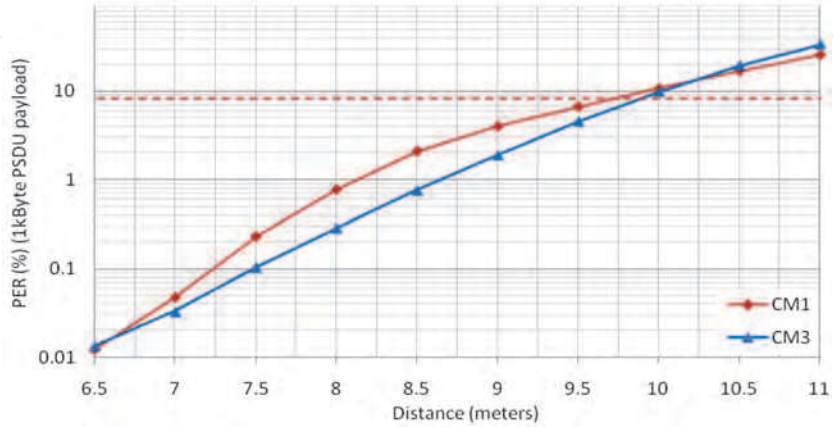

Fig. 10. System performance for 200 Mb/s mode in CM1 and CM3

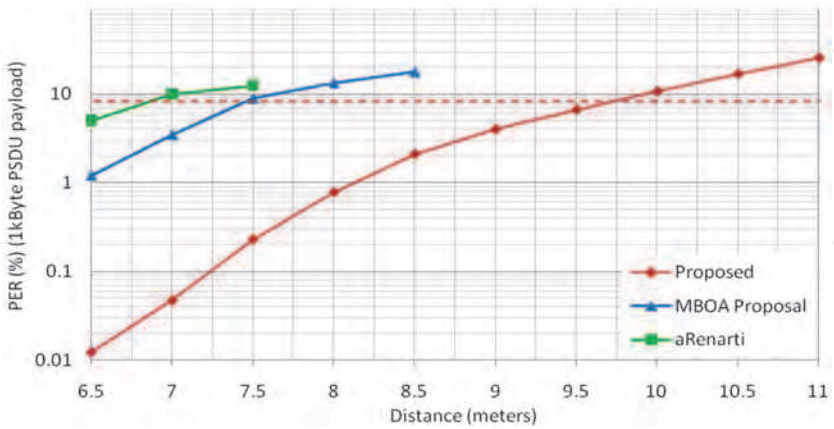

Fig. 11. Performance comparison for 200 Mb/s mode in CM1

4. Dual Carrier Modulation (DCM)

4.1 DCM mapping

DCM as a four-dimensional constellation is used for the highest 3 out of the 8 PSDU coding schemes. After bit interleaving, 1200 interleaved and coded bits are divided into groups of 200 bits, and further grouped into 50 groups of 4 reordering bits. Each group of 4 bits is represented as ($b_{g(k)}$, $b_{g(k)+1}$, $b_{g(k)+50}$, $b_{g(k)+51}$), where $k \in [0\ldots49]$ and

$$g(k) = \begin{cases} 2k & k \in [0\ldots24] \\ 2k+50 & k \in [25\ldots49] \end{cases} \tag{13}$$

These four binary bits are mapped to two QPSK symbols ($x_{g(k)}+jx_{g(k)+50}$), ($x_{g(k)+1}+jx_{g(k)+51}$) as in (14). Then the DCM mapper uses a DCM matrix H as in (15) to execute mapping of the two QPSK symbols into two DCM symbols ($y_{(k)}$, $y_{(k+50)}$) as in (16), where $1/\sqrt{10}$ is a normalization factor for normalizing the average symbol power to be a constant unit. The resulting DCM symbols are formed into two 16-QAM-like constellations, as in Figure 12.

$$\begin{bmatrix} x_{g(k)} + jx_{g(k)+50} \\ x_{g(k)+1} + jx_{g(k)+51} \end{bmatrix} = \begin{bmatrix} (2b_{g(k)} - 1) + j(2b_{g(k)+50} - 1) \\ (2b_{g(k)+1} - 1) + j(2b_{g(k)+51} - 1) \end{bmatrix} \tag{14}$$

$$H = \begin{bmatrix} 2 & 1 \\ 1 & -2 \end{bmatrix} \tag{15}$$

$$\begin{bmatrix} y_{(k)} \\ y_{(k+50)} \end{bmatrix} = \frac{1}{\sqrt{10}} \begin{bmatrix} 2 & 1 \\ 1 & -2 \end{bmatrix} \begin{bmatrix} x_{g(k)} + jx_{g(k)+50} \\ x_{g(k)+1} + jx_{g(k)+51} \end{bmatrix} \tag{16}$$

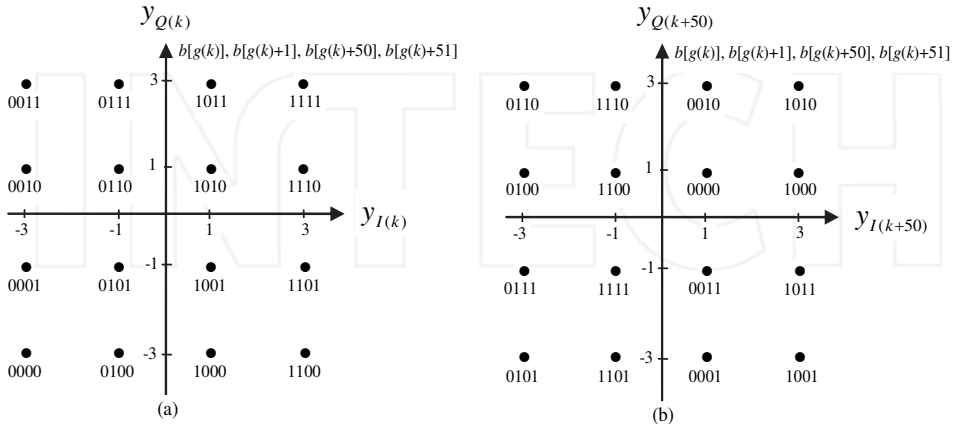

Fig. 12. DCM constellation mapping (ECMA, 2008): (a) mapping for y_k; (b) mapping for y_{k+50}

Information on a single tone is unreliable if a channel has deep fade. If the tone is completely attenuated by the multipath channel, the information will be completely lost. The probability of two tones experiencing a channel deep fade is extremely small if the two tones with the same information are separated by a large bandwidth. Frequency diversity is used in the DCM by mapping the same information but with different forms onto two different tones at different channel frequencies with a large bandwidth separation. The two resulting DCM symbols are allocated into two individual OFDM data subcarriers with 50 subcarriers separation to achieve frequency diversity. 100 DCM symbols (complex numbers) are given to the 128 points IFFT block for building an OFDM symbol. Each OFDM subcarrier occupies a bandwidth of 4.125 MHz (528 MHz/128). Therefore the bandwidth between the two individual OFDM data subcarriers related to the two complex numbers $(I_{(k)}, Q_{(k)})$ and $(I_{(k+50)}, Q_{(k+50)})$ is at least 200 MHz, which offers good frequency diversity gain against channel deep fading. Figure 13 depicts the DCM mapping process.

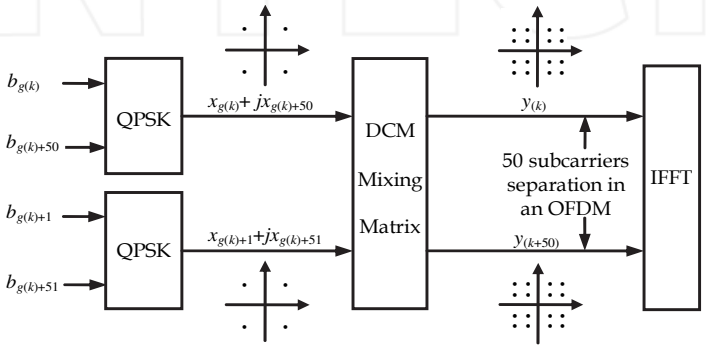

Fig. 13. DCM mapping process

4.2 DCM demapping

The receiver converts each time-domain OFDM symbol into the frequency-domain via the Fast Fourier Transform (FFT). Then, channel estimation and symbol equalization follow. The DCM demapper uses two separate subcarriers concurrently to decode the symbol pair. If one symbol within one subcarrier is lost or degraded, it can be detected, even recovered by the DCM demapper. It is required to repeatedly execute demapping of the two received DCM symbols to output groups of 200 soft bits. The soft bits from the DCM demapper are then input to the bit deinterleaver, the soft bit Viterbi decoder and then descrambled to recover the PSDU, as same as in Figure 6.

4.2.1 Channel State Information

In ECMA-368, the channel estimate section in PLCP preamble is used to form an estimate of the transmission channel, commonly termed the Channel State Information (CSI). It can be used as a dynamic estimation in the frequency-domain for data reliability in each subcarrier position (Li et al., 2005). Each OFDM data subcarrier has a potentially different CSI. The more CSI measurement that can be taken, the more reliable the CSI estimation is in the presence of thermal noise offering better decoding result. The LS algorithm having low complexity to implement is one of the popular methods for the OFDM based system channel estimation

without using any knowledge of the statistics for the channels, as in (17). Furthermore, it has been shown that LS estimation has similar performance close to MMSE (Li et al., 2005).

$$\hat{H}_{LS} = \left(X_k^{-1} Y_k \right) \text{ (k = 0, 1,…)} \tag{17}$$

ECMA-368 defines 6 stored CE sequences (CE0…CE5) in blocks of 122 subcarriers contained in the 6 OFDM symbols of the PLCP preamble in order to simplify the required receiver processing. The proposed LS channel estimator uses the 6 received CE sequences with the priori CE sequences and TFCs to create 6 received merged and inversed CE sequences (channel response) by taking the average of each CE sequence sent on the same frequency. The channel estimator calculates the CE sequence with priori transmitted CE sequence. To maintain the polarity of each received CE value ($CEr = I_{rx\_CE} + jQ_{rx\_CE}$), each received CE value is divided by its expected value that are a priori CE value, CEs. The division is conducted with the stored values at 1+j1, 1-j1, -1+j1, -1-j1, hence a simple look-up table allows each division to easily sum the real part and imaginary part of the received CE value and permuting the polarity of the received CE value, as the following:

$$\begin{aligned} I_{estimated\_CE} + jQ_{estimated\_CE} &= \frac{I_{rx\_CE} + jQ_{rx\_CE}}{1+j} = \frac{(I_{rx\_CE} + Q_{rx\_CE}) + j(Q_{rx\_CE} - I_{rx\_CE})}{2} \\ or \quad &= \frac{I_{rx\_CE} + jQ_{rx\_CE}}{1-j} = \frac{(I_{rx\_CE} - Q_{rx\_CE}) + j(I_{rx\_CE} + Q_{rx\_CE})}{2} \\ or \quad &= \frac{I_{rx\_CE} + jQ_{rx\_CE}}{-1+j} = \frac{(Q_{rx\_CE} - I_{rx\_CE}) - j(I_{rx\_CE} + Q_{rx\_CE})}{2} \\ or \quad &= \frac{I_{rx\_CE} + jQ_{rx\_CE}}{-1-j} = \frac{-(I_{rx\_CE} + Q_{rx\_CE}) + j(I_{rx\_CE} - Q_{rx\_CE})}{2} \end{aligned} \tag{18}$$

Due to the assumption in MB-OFDM that a channel is linear and time invariant over each PPDU (Foerster, 2003), and also that at least 2 of the 6 channel estimation sequences will be on the same carrier frequency, the receiver may average channel estimates from the same carrier frequency to reduce the effect of Gaussian noise. Figure 14 depicts the averaged and inversed CE sequences. For the non-hopping schemes, all the 6 channel estimation bursts $\hat{H}_{CE1} \ldots \hat{H}_{CE6}$ can be averaged together and then inversed for one of the non-hopping schemes in mandatory mode (TFC=1, BG1). Finally, the average received CE sequences are inversed.

$\frac{\hat{H}_{CE1} + \hat{H}_{CE4}}{2}$	$\frac{\hat{H}_{CE2} + \hat{H}_{CE5}}{2}$	$\frac{\hat{H}_{CE3} + \hat{H}_{CE6}}{2}$	$\frac{\hat{H}_{CE1} + \hat{H}_{CE4}}{2}$	$\frac{\hat{H}_{CE2} + \hat{H}_{CE5}}{2}$	$\frac{\hat{H}_{CE3} + \hat{H}_{CE6}}{2}$
⇩					
$\hat{H}_{\overline{CE1}}$	$\hat{H}_{\overline{CE2}}$	$\hat{H}_{\overline{CE3}}$	$\hat{H}_{\overline{CE4}}$	$\hat{H}_{\overline{CE5}}$	$\hat{H}_{\overline{CE6}}$
⇩					
$(\hat{H}_{\overline{CE1}})^{-1}$	$(\hat{H}_{\overline{CE2}})^{-1}$	$(\hat{H}_{\overline{CE3}})^{-1}$	$(\hat{H}_{\overline{CE4}})^{-1}$	$(\hat{H}_{\overline{CE5}})^{-1}$	$(\hat{H}_{\overline{CE6}})^{-1}$
⇩					
H_{CE1}	H_{CE2}	H_{CE3}	H_{CE4}	H_{CE5}	H_{CE6}

Fig. 14. Averaged and inversed channel estimation sequences for TFC=1, BG=1

The CSI is estimated from each of the CE sequences transmitted on that band. The LS CSI for each equalized data is calculated from the received and stored CE sequences and given by (19). It should be noted that CEr/CEs includes both phase and amplitude information, i.e. the I and Q components of each frequency component of the sequences, whereas CSI is the modulus of CEr/CEs and therefore is a scalar term. Moreover, no division is required in the CSI calculation according to (18), where CE_r is the received CE sequence, CE_s is the priori stored CE sequence, which means the divider can be avoided in the hardware implementation, thus lowering the complexity of system implementation.

$$CSI \approx \left| \frac{CE_r}{CE_s} \right| \tag{19}$$

With the similarity of computing the channel estimation, taking the 6 CE sequences can create the 6 averaging blocks of CSI for the non-hopping schemes. Hence, averaging those different blocks of CSI can produce a more accurate CSI in the time invariant or slowly changing channel with respect to the frame time. Again, subject to the mandatory mode, TFC=1 and BG=1 is selected for the band hopping. The first block of CSI is averaged with the fourth block of CSI while the second one is averaged with the fifth one, and the third one is averaged with the sixth one. Then the new averaged CSI blocks are illustrated in Figure 15.

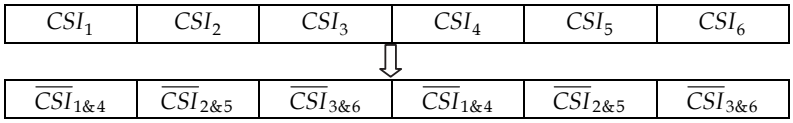

Fig. 15. Averaged CSI blocks allocation for TFC=1, BG=1

To avoid the cost of this CSI aided Viterbi decoder, the soft input of the decoding chain is obtained from the multiplication of the demodulation soft output R_m and its corresponding CSI_k, as described in (20). The receiver is arranged to modify the soft bits using the CSI, as illustrated in Figure 16. The overall data reliability is obtained from directly scaling the soft bit value by the corresponding CSI value. Therefore the reliability of received data is maximized. What is of upmost interest is to apply the CSI as a demapping technique for the MB-OFDM system at the higher data rates, where the DCM modulation scheme is used.

$$Softbit_m = R_m \times CSI_k \tag{20}$$

where m is the index of the numbers of soft bit value depending on the modulation scheme; k is the index into the 100 data subcarriers in an OFDM symbol.

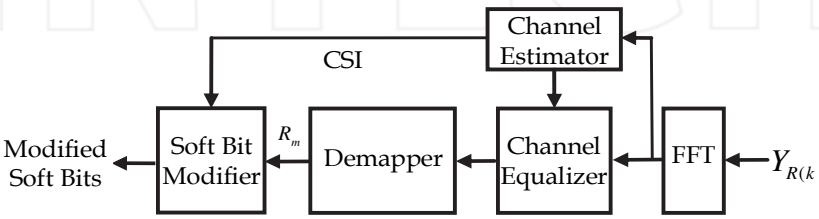

Fig. 16. Demodulation exploiting CSI

4.2.2 Soft bit demapping

The DCM demapper shall demap two equalized complex numbers ($I_{R(k)}$, $Q_{R(k)}$) and ($I_{R(k+50)}$, $Q_{R(k+50)}$) that previously transmitted on two different subcarriers back to two related DCM symbols by using the DCM mixing matrix. Then the DCM demapper outputs the corresponding real part and imaginary part as a group of 4 soft bits, as described in (21)-(24). However, demapping performance can remain the same without using the factor of $\sqrt{10}/5$. The group of 4 soft bits applying two CSI values are from two corresponding data subcarriers in an OFDM symbol, as described in (25)-(28).

$$Soft(b_{g(k)}) = \sqrt{10}\left(2I_{R(k)} - I_{R(k+50)}\right)/5 \tag{21}$$

$$Soft(b_{g(k)+1}) = \sqrt{10}\left(I_{R(k)} - 2I_{R(k+50)}\right)/5 \tag{22}$$

$$Soft(b_{g(k)+50}) = \sqrt{10}\left(2Q_{R(k)} + Q_{R(k+50)}\right)/5 \tag{23}$$

$$Soft(b_{g(k)+51}) = \sqrt{10}\left(Q_{R(k)} - 2Q_{R(k+50)}\right)/5 \tag{24}$$

$$Soft(b_{g(k)}) = \left(2I_{R(k)} + I_{R(k+50)}\right) \times \min\left\{CSI_k, CSI_{k+50}\right\} \tag{25}$$

$$Soft(b_{g(k)+1}) = \left(I_{R(k)} - 2I_{R(k+50)}\right) \times \min\left\{CSI_k, CSI_{k+50}\right\} \tag{26}$$

$$Soft(b_{g(k)+50}) = \left(2Q_{R(k)} + Q_{R(k+50)}\right) \times \min\left\{CSI_k, CSI_{k+50}\right\} \tag{27}$$

$$Soft(b_{g(k)+51}) = \left(Q_{R(k)} - 2Q_{R(k+50)}\right) \times \min\left\{CSI_k, CSI_{k+50}\right\} \tag{28}$$

4.2.3 Maximum likelihood soft bit demapping

The more reliable soft bit values that are given to Viterbi decoder, the more accurately the binary bits can be decoded. Maximum Likelihood (ML) offers finding parameters to obtain the most probable emitted symbols (Oberg, 2001). The DCM symbols are transmitted at different amplitudes and phases (I and Q values). The real part or the imaginary part in the two DCM symbols (signal amplitude) is always fixed with data pairs being -3 and +1, -1 and -3, +1 and +3, +3 and -1. In our case, the large probable soft bit value can be obtained from the two received DCM symbols with an appropriate parameter θ, as described in (29)-(32). The DCM symbol pair, $y_{R(k)}$ and $y_{R(k+50)}$, is received from the channel equalization.

$$Soft(b_{g(k)}) = 2I_{R(k)}\theta + I_{R(k+50)} \tag{29}$$

$$Soft(b_{g(k)+1}) = I_{R(k)} - 2I_{R(k+50)}\theta \tag{30}$$

$$Soft(b_{g(k)+50}) = 2Q_{R(k)}\theta + Q_{R(k+50)} \tag{31}$$

$$Soft(b_{g(k)+51}) = Q_{R(k)} - 2Q_{R(k+50)}\theta \tag{32}$$

To find the appropriate parameter θ, two conditions need to be satisfied.

a. If perfect, I and Q values received are input to the DCM demapper, applying θ to equations (29)-(32) to make the soft magnitude sufficiently large;
b. A symbol in the DCM symbol pair is transmitted with a large magnitude I (or Q), while another symbol in the DCM symbol pair is transmitted with a small magnitude I (or Q). The signal with smaller power can be more easily corrupted. Suppose the small magnitude I (or Q) in a DCM symbol is received as inverted, while the large magnitude I (or Q) in another DCM symbol is received as uncorrupted. In this case, a maximum θ is required to retain the sign of the soft bit value; otherwise using a larger θ can make the sign of the soft bit value inverted, which causes errors for the soft bit decoding.

θ is set to 1.5 as a threshold value according to the two conditions above. The ML soft bit is generated with the appropriate factor and CSI aided technique as described in the following:

$$Soft(b_{g(k)}) = \left(3I_{R(k)} + I_{R(k+50)}\right) \times \min\left\{CSI_k, CSI_{k+50}\right\} \tag{33}$$

$$Soft(b_{g(k)+1}) = \left(I_{R(k)} - 3I_{R(k+50)}\right) \times \min\left\{CSI_k, CSI_{k+50}\right\} \tag{34}$$

$$Soft(b_{g(k)+50}) = \left(3Q_{R(k)} + Q_{R(k+50)}\right) \times \min\left\{CSI_k, CSI_{k+50}\right\} \tag{35}$$

$$Soft(b_{g(k)+51}) = \left(Q_{R(k)} - 3Q_{R(k+50)}\right) \times \min\left\{CSI_k, CSI_{k+50}\right\} \tag{36}$$

4.2.4 Log likelihood ratio demapping

As well as improving the symbol reliability at the input of the Viterbi decoder, Log Likelihood Ratio (LLR) is another alternative demapping approach for the DCM. The generic format of LLR equation can be expressed in (37). In our case, a LLR is calculated from the received DCM symbols $y_{R(k)}$ and $y_{R(k+50)}$. In addition, the LLR functions related to the two 16-QAM like constellations are independent. Hence the LLR for a group of 4 bits ($b_{g(k)}$, $b_{g(k)+1}$, $b_{g(k)+50}$, $b_{g(k)+51}$) is formed from combining the two independent LLR, as in (38)-(41). σ_2 is noise variance associated with the channel.

$$LLR = \log\left(\exp(A) + \exp(B)\right) - \log\left(\exp(X) + \exp(Y)\right) \tag{37}$$

$$\begin{aligned} LLR(b_{g(k)}) = \log & \left\{ \sum_{b_{g(k)}=1} \exp\left[\frac{\left(I_{T(k)} - I_{R(k)}\right)^2}{-\sigma_k^2} \right] + \sum_{b_{g(k)}=1} \exp\left[\frac{\left(I_{T(k+50)} - I_{R(k+50)}\right)^2}{-\sigma_{k+50}^2} \right] \right\} \\ & - \log \left\{ \sum_{b_{g(k)}=0} \exp\left[\frac{\left(I_{T(k)} - I_{R(k)}\right)^2}{-\sigma_k^2} \right] + \sum_{b_{g(k)}=0} \exp\left[\frac{\left(I_{T(k+50)} - I_{R(k+50)}\right)^2}{-\sigma_{k+50}^2} \right] \right\} \end{aligned} \tag{38}$$

$$LLR(b_{g(k)+1}) = \log\left\{\sum_{b_{g(k)+1}=1}\exp\left[\frac{\left(I_{T(k)}-I_{R(k)}\right)^2}{-\sigma_k^2}\right]+\sum_{b_{g(k)+1}=1}\exp\left[\frac{\left(I_{T(k+50)}-I_{R(k+50)}\right)^2}{-\sigma_{k+50}^2}\right]\right\}$$
$$-\log\left\{\sum_{b_{g(k)+1}=0}\exp\left[\frac{\left(I_{T(k)}-I_{R(k)}\right)^2}{-\sigma_k^2}\right]+\sum_{b_{g(k)+1}=0}\exp\left[\frac{\left(I_{T(k+50)}-I_{R(k+50)}\right)^2}{-\sigma_{k+50}^2}\right]\right\} \quad (39)$$

$$LLR(b_{g(k)+50}) = \log\left\{\sum_{b_{g(k)+50}=1}\exp\left[\frac{\left(Q_{T(k)}-Q_{R(k)}\right)^2}{-\sigma_k^2}\right]+\sum_{b_{g(k)+50}=1}\exp\left[\frac{\left(Q_{T(k+50)}-Q_{R(k+50)}\right)^2}{-\sigma_{k+50}^2}\right]\right\}$$
$$-\log\left\{\sum_{b_{g(k)+50}=0}\exp\left[\frac{\left(Q_{T(k)}-Q_{R(k)}\right)^2}{-\sigma_k^2}\right]+\sum_{b_{g(k)+50}=0}\exp\left[\frac{\left(Q_{T(k+50)}-Q_{R(k+50)}\right)^2}{-\sigma_{k+50}^2}\right]\right\} \quad (40)$$

$$LLR(b_{g(k)+51}) = \log\left\{\sum_{b_{g(k)+51}=1}\exp\left[\frac{\left(Q_{T(k)}-Q_{R(k)}\right)^2}{-\sigma_k^2}\right]+\sum_{b_{g(k)+51}=1}\exp\left[\frac{\left(Q_{T(k+50)}-Q_{R(k+50)}\right)^2}{-\sigma_{k+50}^2}\right]\right\}$$
$$-\log\left\{\sum_{b_{g(k)+51}=0}\exp\left[\frac{\left(Q_{T(k)}-Q_{R(k)}\right)^2}{-\sigma_k^2}\right]+\sum_{b_{g(k)+51}=0}\exp\left[\frac{\left(Q_{T(k+50)}-Q_{R(k+50)}\right)^2}{-\sigma_{k+50}^2}\right]\right\} \quad (41)$$

For a Gaussian channel, the LLR can be approximated as two piecewise-linear functions which depend on the amplitude of I/Q signals (Seguin, 2004). Furthermore, the maximum LLR value can be approximated to be soft magnitude with the associated bit completely depending on the amplitude of the I/Q signals. In our case, there are two bits associated with each of the two 16-QAM like constellations completely relying on their soft magnitude of the I/Q. The LLR functions related to these two bits from each constellation are considered to be partially linear. Therefore some terms of these LLR functions are approximated by soft magnitude, as in (42)-(45). The CSI is also used for LLR soft bit values scaling. The noise variance is obtained from mapping the ratio of received symbol and its average energy estimate has been taken into account to approximate the LLR value.

$$LLR(b_{g(k)}) = 3I_{R(k)} + \log\left\{\sum_{b_{g(k)}=1}\exp\left[\frac{\left(I_{T(k+50)}-I_{R(k+50)}\right)^2}{-\sigma_{k+50}^2}\right]\right\}$$
$$-\log\left\{\sum_{b_{g(k)}=0}\exp\left[\frac{\left(I_{T(k+50)}-I_{R(k+50)}\right)^2}{-\sigma_{k+50}^2}\right]\right\} \quad (42)$$

$$LLR(b_{g(k)+1}) = \log\left\{\sum_{b_{g(k)+1}=1} \exp\left[\frac{\left(I_{T(k)} - I_{R(k)}\right)^2}{-\sigma_k^2}\right]\right\} - \log\left\{\sum_{b_{g(k)+1}=0} \exp\left[\frac{\left(I_{T(k)} - I_{R(k)}\right)^2}{-\sigma_k^2}\right]\right\} - 3I_{R(k+50)} \tag{43}$$

$$LLR(b_{g(k)+50}) = 3Q_{R(k)} + \log\left\{\sum_{b_{g(k)+50}=1} \exp\left[\frac{\left(Q_{T(k+50)} - Q_{R(k+50)}\right)^2}{-\sigma_{k+50}^2}\right]\right\} - \log\left\{\sum_{b_{g(k)+50}=0} \exp\left[\frac{\left(Q_{T(k+50)} - Q_{R(k+50)}\right)^2}{-\sigma_{k+50}^2}\right]\right\} \tag{44}$$

$$LLR(b_{g(k)+51}) = \log\left\{\sum_{b_{g(k)+51}=1} \exp\left[\frac{\left(Q_{T(k)} - Q_{R(k)}\right)^2}{-\sigma_k^2}\right]\right\} - \log\left\{\sum_{b_{g(k)+51}=0} \exp\left[\frac{\left(Q_{T(k)} - Q_{R(k)}\right)^2}{-\sigma_k^2}\right]\right\} - 3Q_{R(k+50)} \tag{45}$$

Now the LLR functions have been simplified by approximating with a linear part, to solve the non-linear part for the LLR function, the noise variance σ^2 needs to be estimated, which generally requires the mean of the absolute value of the received symbol components (m, as in (46)) and also estimates the average energy of the received symbol components (E, as in (47)). The ratio of m^2/E can be mapped to ratio a/m (a is signal amplitude, I or Q) and ratio σ^2/m. σ^2 can be determined from this mapping, but requiring large calculation in hardware and computation simulation.

$$m = \frac{1}{2k}\sum_{k=1}^{K}\left\{\left(\left|I_{R(k)}\right| + \left|Q_{R(k)}\right|\right)\right\} \tag{46}$$

$$E = \frac{1}{2k}\sum_{k=1}^{K}\left\{\left(\left|I^2{}_{R(k)}\right| + \left|Q^2{}_{R(k)}\right|\right)\right\} \tag{47}$$

4.2.5 System performance for 480 Mb/s mode

The system is simulated at the data rate of 480 Mb/s in UWB channel model 1 (CM1). The original MB-OFDM proposal settings of 2000 packets per simulation with a payload of 1024 octets each in the PSDU and 90th-percentile channel realization were followed. Strict adherence to timing was used. A hopping characteristic of TFC=1 was used. A 6.6 dB noise figure and a 2.5 dB implementation loss in the floating point system model were incorporated. The guard interval diversity is also used in the simulation.

The system performance exploiting soft bit, ML soft bit, and LLR DCM demapping methods with CSI as demapping enhancements were examined. From the simulation results shown in Figure 17, LLR with CSI is better demapping method and can achieve 3.9 meters in CM1. On closer examination for the performance at 8% PER, ML soft bit demapping method can achieve 3.9 meters in CM1 as well. In this case it is reasonable to conclude that ML soft bit demapping has same performance as LLR, but with slightly worse performance in shorter distance transmission. Soft bit demapping with CSI can only achieve 3.4 meters at 8% PER level in CM1. However soft bit or ML soft bit demapping method has lower computation complexity and reduces hardware implementation cost. Therefore ML soft bit demapping with CSI will be the best demapping method to implement hardware for ECMA-368.
The system performance in the 480 Mb/s mode was compared with current literature. It is difficult to compare the system performance with all the literature because most of them did not follow the conformance testing from WiMedia. This research used the simulation result from MBOA-SIG proposal (Multiband OFDM Alliance, 2004) for comparison. By implementing Kim's LLR DCM demapping method (Kim, 2007) with this proposed CSI further demapping technique, then the research will have the system performance using Kim's method for comparison. Figure 18 depicts the comparision for system performance for 480 Mb/s mode in CM1, wherein a performance gain can be achieved by the proposed LLR CSI method, while the system performance is 3.8 meters in MBOA-SIG proposal and the sytem using Kim's method. As can be seen, the proposed LLR CSI scheme performs the best at 8% PER.

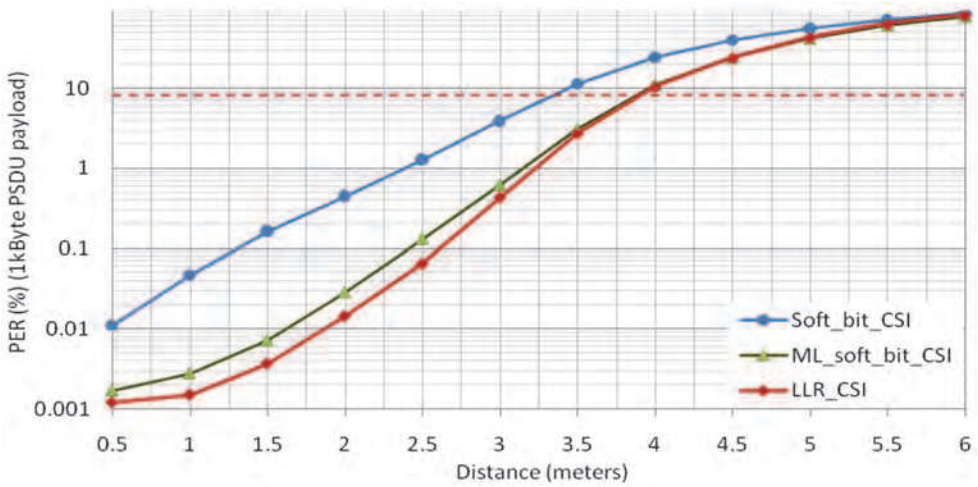

Fig. 17. Performance comparison for the proposed DCM demapping methods

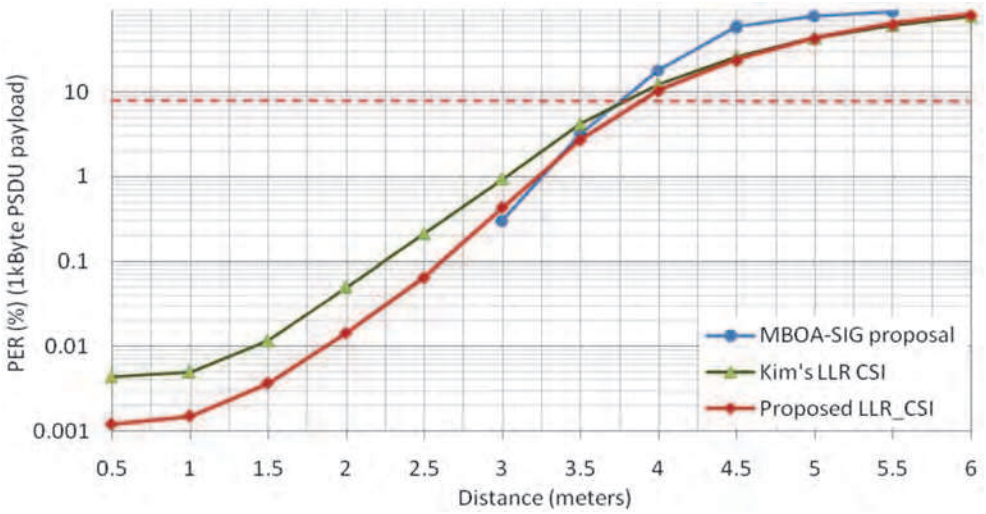

Fig. 18. Performance comparison for 480 Mb/s mode in CM1

4.3 Dual Circular 32-QAM

To enable the transport of high data rate UWB communications, ECMA-368 offers up to 480 Mb/s instantaneous bit rate to the MAC layer. However the maximum data rate of 480 Mb/s in a practical radio environment can not be achieved due to poor radio channel conditions causing dropped packets unfortunately resulting in a lower throughput hence need to retransmit the dropped packets. An alternative high data rate modulation scheme is needed to allow effective 480 Mb/s performance.

Two 16-QAM-like constellation mappings are used in the DCM. Obviously if only one 16-QAM-like constellation mapping is used for the modulation, this would result in less reliability but twice the number of bits can be transmitted per subcarrier offering faster throughput, which is from 640 Mb/s to 960 Mb/s comparing to DCM 320 Mb/s to 480 Mb/s mode (see Table 3). However there is no successful link under multipath environments (CM1...CM4) transmitting at 960 Mb/s or the system has poor performance only achieving 1.2 meters at 640 Mb/s. The simulation result will be shown in section 4.3.3. Hence 16-QAM is not the ideal modulation scheme for the high data rate MB-OFDM system.

4.3.1 Dual Circular 32-QAM mapping

Since 16-QAM is not a suitable modulation scheme for the high data rate MB-OFDM system, there is no need to consider higher order modulations, for instance 32-QAM, 64-QAM etc. Therefore if a new modulation scheme is proposed to fit into the existing system, the new modulation scheme comprising for an OFDM symbol shall not map the number of bits over 400 bits. Moreover, the new modulation scheme needs to be robust mapping 400 bits or less with successful transmission in a multipath environment.

A Dual Circular (DC) 32-QAM modulator is proposed to use two 8-ary PSK-like constellations mapping 5 bits into two symbols, which is basically derived from two QPSK symbols mapping 4 bits and taken the bipolarity of the fifth bit to drive the two QPSK

constellations to two 8-ary PSK-like constellations. Within a group of 5 bits, the first and second bit are mapped into one DC 32-QAM symbol, while the third and forth bit are mapped into another DC 32-QAM symbol, and then the fifth bit is mapped into both DC 32-QAM symbols offering diversity. 250 interleaved and coded bits are required to map by the DC 32-QAM mapper onto 100 data subcarriers in an OFDM symbol, hence increasing the system throughput to 600 Mb/s comparing to the DCM 480 Mb/s mode (see Table 3).
Figure 19 depicts the proposed DC 32-QAM modulator as an alternative modulation scheme that fits into the existing PSDU encoding process with the objective to map more information bits onto an OFDM symbol. After the bit interleaving, 1500 coded and interleaved bits are required to divide into groups of 250 bits and then further grouped into 50 groups of 5 reordering bits. Each group of 5 bits is represented as ($b_{g(k)}$, $b_{g(k)+50}$, $b_{g(k)+51}$, $b_{g(k)+100}$, $b_{g(k)+101}$), where $k \in [0\ldots49]$ and

$$g(k) = \begin{cases} 2k & k \in [\,0\ldots24] \\ 2k+50 & k \in [\,25\ldots49] \end{cases} \tag{48}$$

Four bits ($b_{g(k)+50}$, $b_{g(k)+51}$, $b_{g(k)+100}$, $b_{g(k)+101}$) are mapped across two QPSK symbols ($x_{g(k)}+jx_{g(k)+50}$), ($x_{g(k)+1}+jx_{g(k)+51}$) as in (49). Those two bits pairs are not in consecutive order within the bit streams. $b_{g(k)+50}$ and $b_{g(k)+100}$ are mapped to one QPSK symbol while $b_{g(k)+51}$ and $b_{g(k)+101}$ are mapped to another, which aids to achieve further bit interleaving against burst errors.

Data Rate (Mb/s)	Modulation	Coding Rate (R)	Frequency Domain Spreading	Time Domain Spreading	Coded Bits / 6 OFDM symbol(N_{CBP6S})
53.3	QPSK	1/3	YES	YES	300
80	QPSK	1/2	YES	YES	300
106.7	QPSK	1/3	NO	YES	600
160	QPSK	1/2	NO	YES	600
200	QPSK	5/8	NO	YES	600
320	DCM	1/2	NO	NO	1200
400	DCM	5/8	NO	NO	1200
480	DCM	3/4	NO	NO	1200
600	DC 32-QAM	3/4	NO	NO	1500
640	16-QAM	1/2	NO	NO	2400
960	16-QAM	3/4	NO	NO	2400

Table 3. PSDU rate-dependent parameters

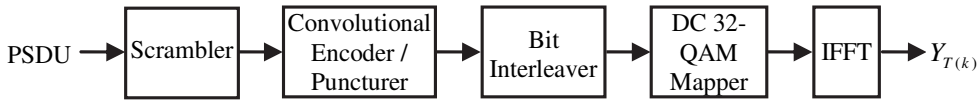

Fig. 19. PSDU Encoding process with DC 32-QAM

$$\begin{bmatrix} x_{g(k)} + jx_{g(k)+50} \\ x_{g(k)+1} + jx_{g(k)+51} \end{bmatrix} = \begin{bmatrix} (2b_{g(k)+50} - 1) + j(2b_{g(k)+100} - 1) \\ (2b_{g(k)+51} - 1) + j(2b_{g(k)+101} - 1) \end{bmatrix} \tag{49}$$

Then these two QPSK symbols are mapped into two DC 32-QAM symbols ($y_{T(k)}$, $y_{T(k+50)}$) depending on value of bit $b_{g(k)}$ as in (50)-(52), where $K_{MOD} = 1/\sqrt{6.175}$ as the normalization factor. Each DC 32-QAM symbol in the constellation mapping has equal decision region for each bit, as illustrated in Figure 20. The DCM symbols having two 16-QAM-like constellations do not have fixed amplitude. Thus the DCM will worsen the Peak to Average Power Ratio (PAPR) of the OFDM signals, resulting in more impact to the Automatic Gain Control (AGC) and ADC. In contract, the constellation points are positioned in circular loci to offer constant power for each DC 32-QAM symbol, which is of great benefit to the AGC and ADC.

$$\begin{bmatrix} y_{T(k)} \\ y_{T(k+50)} \end{bmatrix} = K_{MOD} \begin{bmatrix} \alpha x_{g(k)} + j\beta x_{g(k)+50} \\ \beta x_{g(k)+1} + j\alpha x_{g(k)+51} \end{bmatrix} \tag{50}$$

where

$$\alpha = \begin{cases} 1 & , b_{g(k)} = 0 \\ 2.275 & , b_{g(k)} = 1 \end{cases} \tag{51}$$

$$\beta = \begin{cases} 2.275 & , b_{g(k)} = 0 \\ 1 & , b_{g(k)} = 1 \end{cases} \tag{52}$$

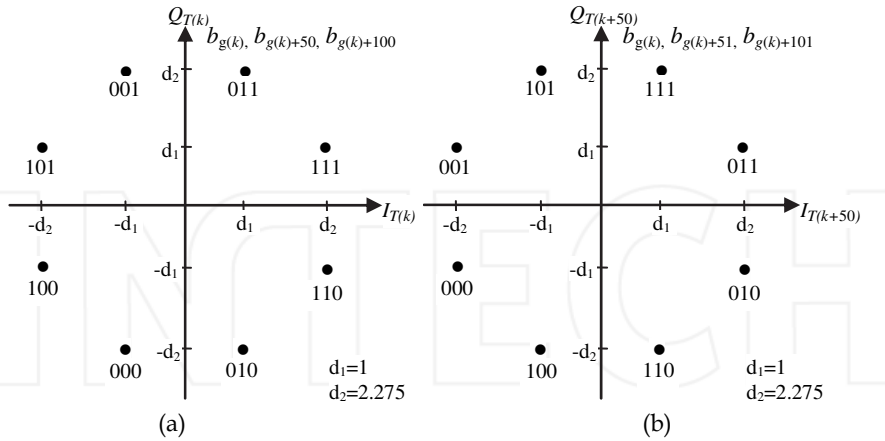

Fig. 20. DC 32-QAM constellation mapping: (a) mapping for $y_{T(k)}$; (b) mapping for $y_{T(k+50)}$

The two resulting DC 32-QAM symbols ($y_{(k)}$, $y_{(k+50)}$) are allocated into two individual OFDM data subcarriers with 50 subcarriers separation to achieve frequency diversity. An OFDM symbol is formed from the 128 point IFFT block requiring 100 DC 32-QAM symbols. Each OFDM subcarrier occupies a bandwidth of about 4 MHz, therefore the bandwidth between

the two individual OFDM data subcarriers related to the two complex numbers ($I_{(k)}$, $Q_{(k)}$) and ($I_{(k+50)}$, $Q_{(k+50)}$) is at least 200 MHz, which offers a frequency diversity gain against channel deep fading. This will benefit for recovering the five information bits mapped across the two DC 32-QAM symbols. Figure 21 depicts the DC 32-QAM mapping process.

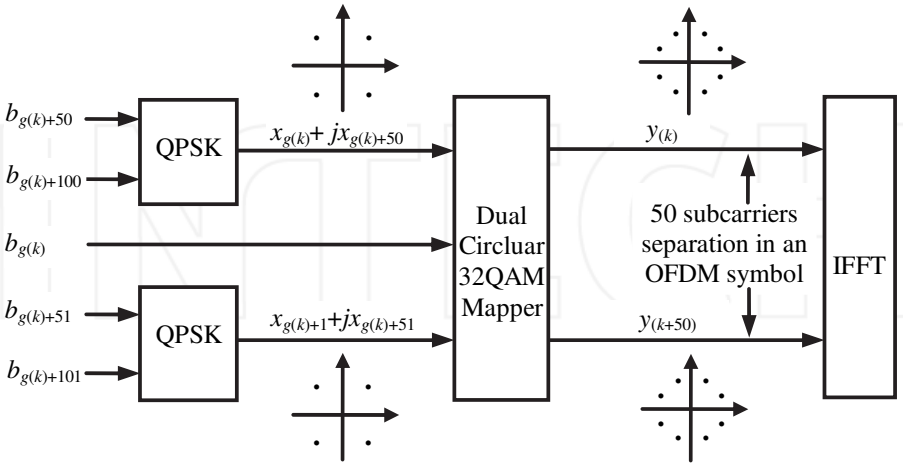

Fig. 21. DC 32-QAM mapping process

4.3.2 DC 32-QAM demapping

The proposed DC 32-QAM utilizes soft bit demapping to demap two equalized complex numbers previously transmitted on different data subcarriers into a subgroup of 5 soft bits, and then outputs groups of 250 soft bits in sequential order. The demapper is proposed to use the DC 32-QAM demapper, and other functional blocks are remained. The demapped and deinterleaved soft bits are input to Viterbi decoder to recover the original bit streams.

Each soft bit value of $b_{g(k)+50}$, $b_{g(k)+51}$, $b_{g(k)+100}$ and $b_{g(k)+101}$ depend on the soft bit magnitude of the I/Q completely. In addition, each soft bit can be demapped from its associated ($I_{R(k)}$, $Q_{(k)}$) and ($I_{R(k+50)}$, $Q_{R(k+50)}$) independently. Furthermore, the demapping performance can remain without using the factor 1/ K_{MOD}. Hence the soft bit values for $b_{g(k)+50}$, $b_{g(k)+51}$, $b_{g(k)+100}$ and $b_{g(k)+101}$ are given by the following.

$$Soft(b_{g(k)+50}) = I_{R(k)} \tag{53}$$

$$Soft(b_{g(k)+51}) = I_{R(k+50)} \tag{54}$$

$$Soft(b_{g(k)+100}) = Q_{R(k)} \tag{55}$$

$$Soft(b_{g(k)+101}) = Q_{R(k+50)} \tag{56}$$

To demap $b_{g(k)}$ in the constellation for $y_{R(k)}$, the demapped information bit is considered to be '1' if the received symbol is close to the constellation point along with I axis, otherwise it is '0' if close to the constellation point along with Q axis. However, to demap $b_{g(k)}$ in the

constellation for $y_{R(k+50)}$, the demapped information bit is considered to be '0' if the received symbol is close to the constellation point along with I axis, otherwise it is '1' if close to the constellation point along with Q axis. Figure 22 depicts Euclidean distances for a possible received DC 32-QAM symbol pair with region for $b_{g(k)}$. Since the bit regions of $b_{g(k)}$ in the two constellation mapping are different, the associated I and Q value from $y_{R(k)}$ and $y_{R(k+50)}$ cannot be simply combined. Hence the Euclidean symbol distance for each received symbol in the associated constellation mapping is calculated first, as in (57)-(60). Then the two Euclidean symbol distances are summed together as a soft bit value for $b_{g(k)}$, as in (61).

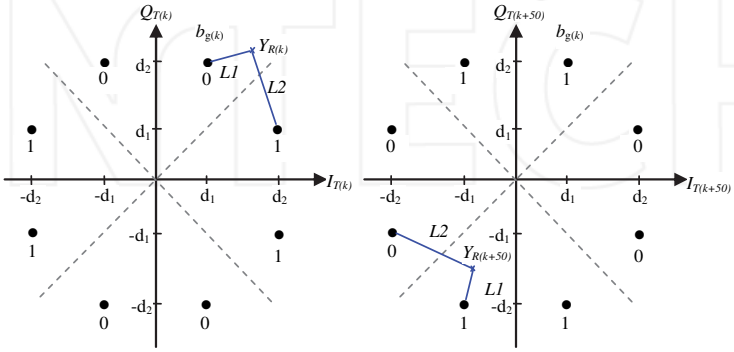

Fig. 22. Symbol distances for a possible received symbol pair $y_{R(k)}$ and $y_{R(k+50)}$ with decision region for $b_{g(k)}$

$$L1 = \sqrt{\left(\left|I_{R(k)}\right| - d1\right)^2 + \left(\left|Q_{R(k)}\right| - d2\right)^2} \tag{57}$$

$$L2 = \sqrt{\left(\left|I_{R(k)}\right| - d2\right)^2 + \left(\left|Q_{R(k)}\right| - d1\right)^2} \tag{58}$$

$$L3 = \sqrt{\left(\left|I_{R(k+50)}\right| - d1\right)^2 + \left(\left|Q_{R(k+50)}\right| - d2\right)^2} \tag{59}$$

$$L4 = \sqrt{\left(\left|I_{R(k+50)}\right| - d2\right)^2 + \left(\left|Q_{R(k+50)}\right| - d1\right)^2} \tag{60}$$

$$Soft(b_{g(k)}) = \frac{1}{2} \times (L1 - L2 + L3 - L4) \tag{61}$$

The proposed CSI aided scheme coupled with the band hopping information maximizes the DCM soft demapping performance. $b_{g(k)}$ mapped to two DC 32-QAM symbols are mapped onto two OFDM data subcarriers resulting in two CSI from the two associated data subcarriers. If a smaller or larger CSI value is chosen as a reliable scale term, it causes inequality of signal power for the different OFDM data subcarriers. The averaging CSI is adopted for $b_{g(k)}$. Therefore the soft bits incorporated with CSI for the DC 32-QAM demapping are given by the following:

$$Soft(b_{g(k)}) = \left(\frac{L1 - L2 + L3 - L4}{2}\right) \times \left(\frac{CSI_k + CSI_{k+50}}{2}\right) \quad (62)$$

$$Soft(b_{g(k)+50}) = I_{R(k)} \times CSI_k \quad (63)$$

$$Soft(b_{g(k)+51}) = I_{R(k+50)} \times CSI_{k+50} \quad (64)$$

$$Soft(b_{g(k)+100}) = Q_{R(k)} \times CSI_k \quad (65)$$

$$Soft(b_{g(k)+101}) = Q_{R(k+50)} \times CSI_{k+50} \quad (66)$$

4.3.3 System performance comparison for 16-QAM, DC 32-QAM and DCM

The system simulation setting is same as in section 4.2.4. To compare 16-QAM, DC 32-QAM and DCM performance, the system is set to the same configuration with the same coding rate. All the modulation schemes for the comparison use the best demapping solutions with CSI aided demapping scheme as presented in this thesis. While changing the modulation scheme and the associated bit interleaver, the system throughput can be increased to 600 Mb/s and 960 Mb/s by DC 32-QAM and 16-QAM respectively, while the DCM performs 480 Mb/s. As shown in Figure 23, there is no successful link if the system is operated with 16-QAM at the data rate of 960 Mb/s. Alternatively lowering the data rate to 640 Mb/s by changing the coding scheme (Table 3), the system performance is only 1.2 meters. However, implementing the DC 32-QAM scheme offers 3.2 meters at 600 Mb/s while the existing system using DCM can be achieved 3.9 meters at 480 Mb/s. The effective 600 Mb/s performance in practical multipath environment with moderate packet loss can offer an effective data rate at 480 Mb/s.

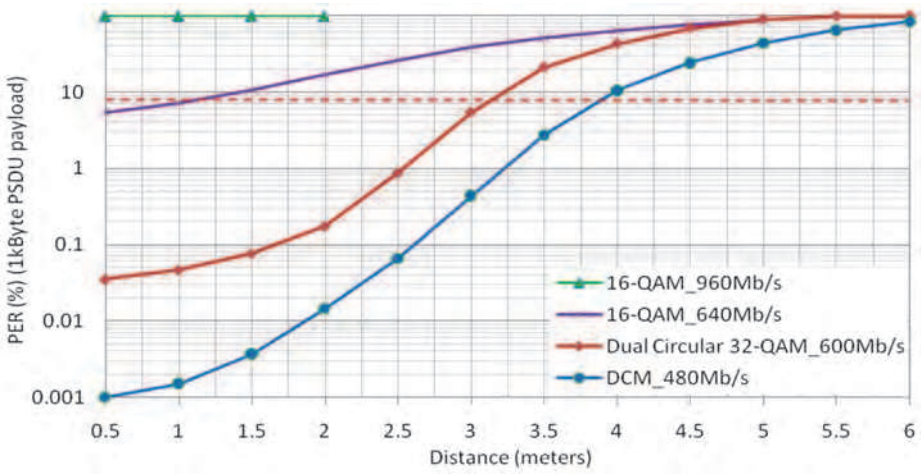

Fig. 23. System performance comparison for 16-QAM, DC 32-QAM and DCM

5. Conclusions

WiMedia Alliance working with ECMA established MB-OFDM UWB radio platform as the global UWB standard, ECMA-368. It is an important part to consumer electronics and the users' experience of these products. Since the standard has been set for the transmitter, optimization of the receiver becomes paramount to maximize the MB-OFDM system performance. Furthermore, the solutions of improving the MB-OFDM need to be cost-effective for implementing the low power and high performance device.

OFDM modulation is the important part for the multicarrier system. The proposed dual QPSK soft demapper exploiting TDS and guard interval diversity improved the system performance with requiring no overhead for ECMA-368. Three DCM demapping methods have been described and developed, which are soft bit demapping, ML soft bit demapping and LLR demapping methods. A CSI aided scheme coupled with the band hopping information maximized the DCM demapping performance, thus improving the system performance. Based on the QPSK and DCM, a cost-effective and high performance modulation scheme (termed DC 32-QAM) that fits within the configuration of current standard offering high rate USB throughput (480 Mb/s) with a moderate level of dropped packets, and can even offer a faster throughput for comparable propagation conditions. The contribution of this research can enable the UWB technology and help to ensure its success.

Hardware implementation at FPGA need solutions for ever increasing demands on system clock rates, silicon performance and long verification times etc. Not only logic and design size minimization, but also architecture solutions will be the challenge for the further research to handle large amounts of data through a fast UWB wireless connection.

6. References

aRenarti Semiconductor (2007). MB-OFDM UWB PHY: Baseband Processor (BBP), August 2007, Available from http://www.arenarti.com/docs/tb1000rB.pdf

Batra, A.; et al. (2004). Multi-band OFDM physical layer proposal for IEEE 802.15 task group 3a, *IEEE standard proposal P802.15-03*, March 2004

Batra, A.; Balakrishnan, J.; Aiello, G.; Foerster, J. & Dabak, A. (2004). Design of a multiband OFDM system for realistic UWB channel environments, *IEEE Transactions on Microwave Theory and Techniques*, Vol.52, No.9, (September 2004), pp 2123-2138, ISSN: 0018-9480

ECMA-368 (2008). High rate ultra wideband PHY and MAC standard (3rd Edition), ECMA International, December 2008

Ellis, J.; Siwiak, K. & Roberts, R. (2002). TG3a Technical Requirements, *IEEE P802.15-03/030-SG3a*, December 2002

FCC (February 2002). New public safety applications and broadband internet access among uses envisaged by FCC authorization of ultra-wideband technology, press released February 14, 2002

FCC (April 2002). Revision of Part 15 of the Commissions Rules Regarding Ultra-Wideband Transmission Systems. *ET Docket 98-153, FCC 02-48*; Released: April 22, 2002

Fisher, R.; et al (2005). DS-UWB Physical Layer Submission to 802.15 Task Group 3a, *IEEE standard proposal IEEE P802.15-04/0137r4*, January 2005

Foerster, J. (2003). Channel Modeling Sub-committee Report Final, *IEEE P802.15-02/490-SG3a*. February 7, 2003

Kim, Y. (2007). Dual Carrier Modulation (DCM) demapping method and demapper, *European Patent Application*, EP1858215A1, November 21, 2007

Li, W.; Wang, Z.; Yan, Y. & Tomisawa, M. (2005). An efficient low-cost LS equalization in COFDM based UWB systems by utilizing channel-state-information (CSI), *IEEE 62nd Vehicular Technology Conference*, Vol. 4, pp. 67-71, ISSN 1090-3038, Dallas, Texas, USA, September 2005,

Multiband OFDM Alliance (2004). MultiBand OFDM Physical Layer Proposal for IEEE 802.15.3a, *IEEE P802.15 Working Group for Wireless Personal Area Networks (WPANs)*. September 2004

Oberg, T. (2001). *Modulation, Detection and Coding*, John Wiley & Sons, ISBN 0471497665, Chichester, England

Proakis, J. G. (2001). *Digital Communications (Fourth edition)*, McGraw-Hill, ISBN 0072321113, New York, USA

Seguin, F.; Lahuec, Lebert, C. J.; Arzel, M. & Jezequel, M. (2004). Analogue 16-QAM demodulator, *IEE Electronics Letters*, Vol.40, No.18, (September 2004), pp.1138-1140, ISSN: 0013-5194

USB Implementers forum (2005). Wireless Universal Serial Bus Specification, Revision 1.0, May 12, 2005

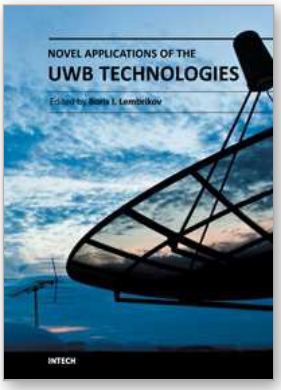

Novel Applications of the UWB Technologies

Edited by Dr. Boris Lembrikov

ISBN 978-953-307-324-8
Hard cover, 440 pages
Publisher InTech
Published online 01, August, 2011
Published in print edition August, 2011

Ultra wideband (UWB) communication systems are characterized by high data rates, low cost, multipath immunity, and low power transmission. In 2002, the Federal Communication Commission (FCC) legalized low power UWB emission between 3.1 GHz and 10.6 GHz for indoor communication devices stimulating rapid development of UWB technologies and applications. The proposed book Novel Applications of the UWB Technologies consists of 5 parts and 20 chapters concerning the general problems of UWB communication systems, and novel UWB applications in personal area networks (PANs), medicine, radars and localization systems. The book will be interesting for engineers and researchers occupied in the field of UWB technology.

INTECH
open science | open minds

InTech Europe
University Campus STeP Ri
Slavka Krautzeka 83/A
51000 Rijeka, Croatia
Phone: +385 (51) 770 447
Fax: +385 (51) 686 166
www.intechopen.com

InTech China
Unit 405, Office Block, Hotel Equatorial Shanghai
No.65, Yan An Road (West), Shanghai, 200040, China
中国上海市延安西路65号上海国际贵都大饭店办公楼405单元
Phone: +86-21-62489820
Fax: +86-21-62489821